International Journal of Heat and Mass Transfer 126 (2018) 342–352

Contents lists available at ScienceDirect

International Journal of Heat and Mass Transfer

journal homepage: www.elsevier.com/locate/ijhmt

The modeling of the formation of technogenic thermal pollution zones in large reservoirs

T. Lyubimova [a,b,*], A. Lepikhin [c], Ya. Parshakova [a], Yu. Lyakhin [c], A. Tiunov [c]

[a] Computational Fluid Dynamics Laboratory, Institute of Continuous Media Mechanics UB RAS, Perm, Russia
[b] Theoretical Physics Department, Perm State University, Perm, Russia
[c] Surface Hydrology Laboratory, Mining Institute UB RAS, Perm, Russia

ARTICLE INFO

Article history:
Received 5 March 2018
Received in revised form 23 April 2018
Accepted 3 May 2018

ABSTRACT

Thermal pollution of water bodies is an unavoidable consequence of thermal or nuclear power plant operation. To minimize the detrimental effects of these plants, one should assess the nature of dangerous zones. The most effective approach to solving these problems is the computational experiment. This paper presents the results of a numerical study of thermal pollution in one of the largest thermal power plants of Europe - Permskaya TPP, using the Kama Reservoir as a natural cooling system. Such problems are traditionally solved in 2D formulation using the "shallow water" approximation. However, with this approach it is impossible to take into account the vertical inhomogeneity of the temperature field. On the other hand, 3D models, which can take into account the effect of density stratification, require very large computational resources. In this work, a combined approach, based on a combination of computational models in the 1D, 2D and 3D formulations, is applied.

1. Introduction

Today, water basins are the most widely used types of cooling systems for large thermal and nuclear power plants. Their exploitation often involves considerable problems peculiar to a particular basin [1–3]. For small cooling basins the problems are associated with the operating limits of a power plant related to a rise of the temperature of water withdrawn from the reservoir [4], whereas for large cooling systems the problems are related to thermal pollution, changes in the ice-thermal regime, hydrophysical and hydrobiological processes, especially in the areas of discharging heated water [5,6]. A key to the solution of a variety of technological and ecological problems is getting the comprehensive and reliable estimates of the parameters of temperature fields generated by these discharges in relation to the technological and hydrometereological parameters [7,8]. The necessary condition for solving the problem of technological and environmental constraints associated with the detrimental impacts of power plants on water bodies is gaining complete and detailed information on the temperature fields in various meteorological and hydrological conditions.

The significance of the problem under consideration is determined by the fact that it came into the view of researchers in early 30-ies of the XX century giving impetus to the development of the first applied models of "plane" hydrodynamics. There are several reasons why finding solutions to these problems is a challenging task. Among the most important complicating factors are the fractality of morphometry of natural water bodies, considerable difference in the scales of natural and technological parameters, and essential variability of hydrometereological factors. Generally, as shown in [9], the coastline represents a fractal and therefore, even a significant refinement of the computational mesh does not give an equivalent increase in the efficiency of the approximation.

Earlier, the restricted efficiency of the computing facilities was one of the main limiting factors. The most widely used approach to these problems was 2D modeling based on the shallow water approximation (see, for example [10–14]). In [9], the authors describe the methods of computational hydrodynamics, which are based on 1- and 2-D modeling. The compact finite difference methods are described in [11]. In [12], a model of sea ice motion, taking into account the atmospheric and water flows due to temperature inhomogeneities, is constructed based on the data of temperature monitoring in the Arctic and Antarctic regions. A 2D-numerical simulation of the spread of thermal pollution in the coastal area of the Red Sea is performed in [13]. An effect of thermal pollution produced by the Iran thermal power plant is numerically investigated in [14] using the 2D approach. Consideration is given to different weather scenarios and temperatures.

However, numerous data of field observations generated the need for revising the formulation which is based on the

* Corresponding author at: Institute of Continuous Media Mechanics, Ural Branch of RAS, Perm, Russia.
E-mail address: lubimova@psu.ru (T. Lyubimova).

https://doi.org/10.1016/j.ijheatmasstransfer.2018.05.017
0017-9310/

two-dimensional representation of the examined fields and homogeneity of the depth distribution of water temperature. Therefore, to obtain reliable results, it is necessary to use a 3D model. In [15–19], the problems of thermal pollution are solved in the framework of such models. Apukhtin et al. [15], the maximum temperature of water in the Beloyarsk reservoir (Russia) was computed using a in-house code, in which the equations of hydrodynamics in the hydrostatic approximation and the energy equation in the 3D approximation are solved by the finite difference method. In [16], a three-dimensional computational package of hydrodynamics (MIKE 3) is used to calculate the temperature field and flows in the East –River river (New-York)) generated under the influence of two thermal power plants (TPP). The computational grid composed of triangular elements was refined near the hot water discharge. An estimate of the maximum water discharge for the worst-case pollution scenario was obtained.

The importance of appropriate resolution of spatial models for correct estimation of the propagation of thermal pollution in rivers is discussed in [17]. In [18] the authors discuss the possibility of combining the models of one-dimensional (1D) and three-dimensional (3D) approximations for studying thermal pollution in lakes caused by a single source.

In works [19–21], a three dimensional numerical simulation of turbulent mixing of water layers of different temperatures was carried out based on the solution of the Navier-Stokes equations and LES approach. Computations were done using a three – stage scheme with parallelization. The computational aspects of the LES approach were discussed in [22–24].

The results of three-dimensional numerical simulation of thermal pollution spreading from the cross flow in the river are presented in paper [25]. The dependence of jet inclination on the depth of the main stream was investigated.

In this paper, with reference to the Permskaya thermal power plant, which is one of the most powerful thermal power plants in Europe, we investigated the temperature fields generated due to a discharge of heated waters taking into account the technological and hydrometeorological parameters.

2. Methodology

2.1. In-situ measurements

The Permskaya TPP is situated on the left bank of the Kama reservoir 5 km upstream from the city of Dobryanka and 60 km upstream of the Kamskaya hydropower plant (Kamskaya HPP) dam. Water is supplied from the Kama reservoir through the intake channel and is withdrawn back into reservoir through the discharged channel (Fig. 1). According to technical specifications, the capacity of the thermal power plant must be as large as 4800 thousand kilowatt (6 power generating units, each of 800 thousands kW). Three power units of total capacity of 2400 thousand kW equipped with a direct cooling system are currently in operation. The projected series of studies based on the computational experiments were aimed at minimizing the possible adverse environmental and technological impacts when choosing the optimal cooling schemes for the power units under development.

The Kama reservoir is morphologically a relatively shallow-water zone, in which the average depth does not exceed 4–7 m. Water from the reservoir is carried out through the water intake channel (2.3 km long) and is withdrawn into the reservoir through the discharge channel (900 m long). The width of the reservoir is about 4.0 km. The inundated bed of the Kama river runs along the opposite bank, where the maximum depth is as large as 23 m (Fig. 2).

The most important parameter for restricting water usage in the examined region of the reservoir is the maximum temperature in the area of operation of the Permskaya TPP. According to the Water Code of the Russian Federation, it is not permitted to increase the temperature of water in surface water bodies due to the thermal discharges by more than 5 °C, in comparison with the natural background temperature. Therefore, it is important to identify the zones with maximum temperature for the hottest period of the year. In this context, the procedure for evaluating the specific features of zones, which may experience thermal pollution during operation of the Permskaya TPP, was implemented in two steps. At the first stage the parameters of temperature fields generated by the discharge of heated TPP water were estimated based on the in-situ measurements and the schemes of model calculations were developed. The second-stage study concerned the verification of the computational models and the implementation of the developed computational schemes to different scenarios.

In-situ investigations were carried out in the Kama reservoir domain 16 km in length. The upper boundary of this region was 3 km upstream from the intake channel, and its lower boundary was 10 km downstream from the mouth of the discharge channel.

A digital relief model (DRM) of the reservoir bottom and its parts was constructed at a scale of 1:10000 for the normal water level at the Kamskaya HPP (108.5 m.abs.) using a professional surveying system. This system consists of a single beam Hydrobox echosounder, a set of Topcon GR-5 GPS GNSS Glonass receivers, and a hydrographical survey software package AquaScanOfficeGG+. Based on the obtained results, a schematic map of the examined area of the reservoir was constructed (Fig. 2).

During the field surveys, temperature measurements were made across the area of the Kama reservoir and through its depth under different meteorological conditions and operating conditions of the Permskaya TPP. The temperature was measured at 1 m-depth increment with the WTW conductivity meters ProfiLineCond 1970i at 16 measurement lines. The measurement points are shown in Fig. 3. Daily processing of a great body of data provided information on the distribution of temperature over the Kama reservoir and through its depth in the region of the Permskaya TPP under specific weather conditions (Figs. 4 and 5).

Meteorological data such as air temperature, wind direction and velocity, humidity, and pressure were recorded (at a 5 min recording interval) in the automatic mode using a Kestrel 4500 portable field meteostation.

Curves of temperature variation with the depth of the water body were plotted in Fig. 5.

2.2. Combined computational approach

In the presence of vertical density stratification, three-dimensional effects play a crucial role in the water dynamics. However, even with the use of modern computational resources, it is impossible to construct a three-dimensional mesh for modeling these effects with sufficient resolution for large water bodies of hundreds of kilometers in length and tens of meters in depth. The development of the combined models may be thought as an effective way to overcome this difficulty. We developed a combined approach including the in-situ measurements and the 1D-, 2D, and 3D numerical simulations. In this approach, the results of 1D modeling are used to formulate boundary conditions for the 2D problem and the results of the 2D modeling are used to formulate boundary conditions for the 3D problem. Solution of a number of important environmental problems solved successfully using this approach [26–29] confirmed that it makes possible to gain information on the considered ecosystem state very quickly which allows to provide effective control of the power plants and prevention of technological and environmental risks.

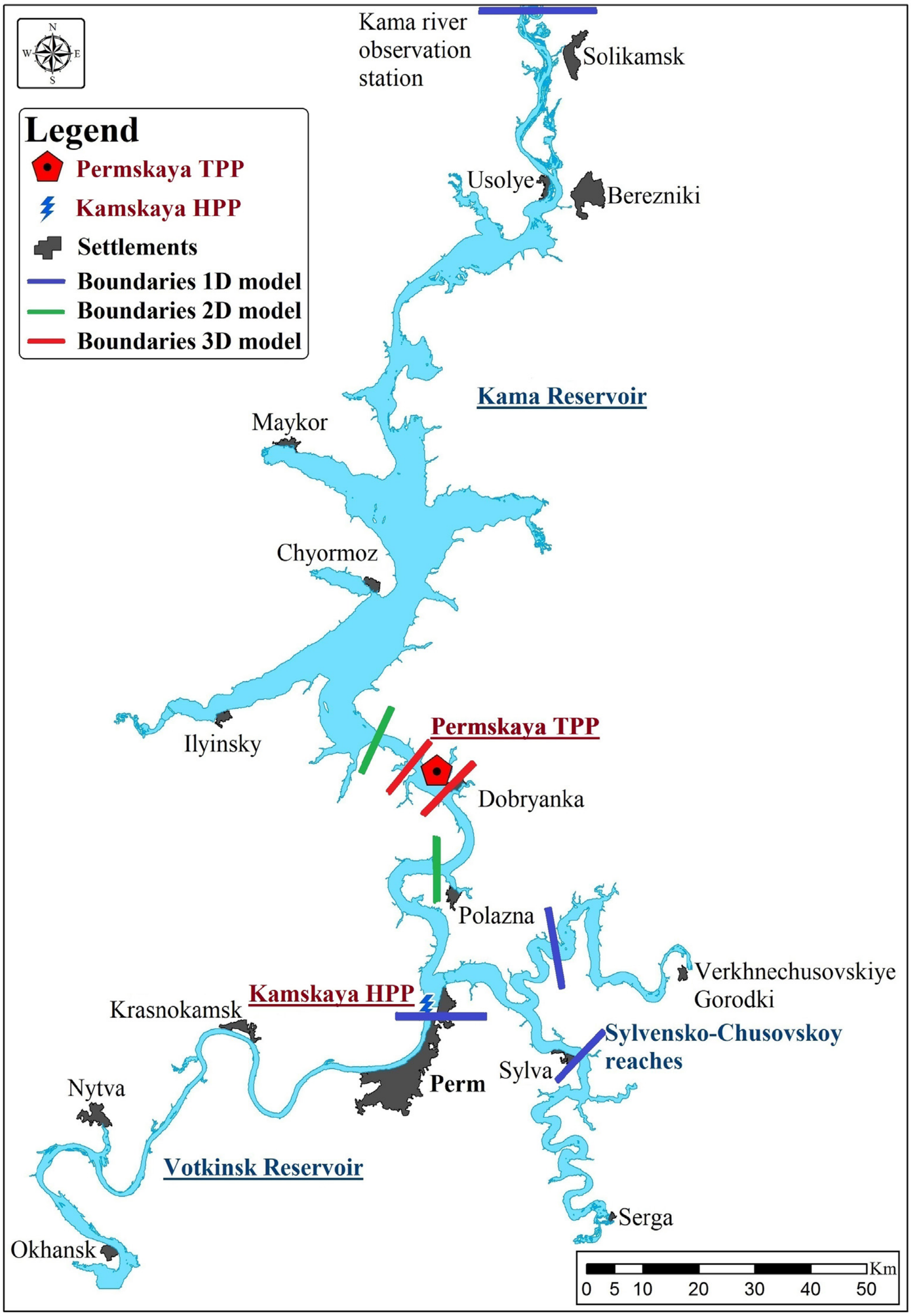

Fig. 1. Location map of the Permskaya TPP in the area of the Kama reservoir.

3. Numerical simulation techniques

3.1. 1D/2D simulations

The regions subject to thermal effects produced by the Permskaya TPP were modeled using the computational scheme that combines 1D, 2D and 3D models. This scheme was chosen due to the significant inhomogeneity of temperature fields across the water area of the Kama reservoir and through its depth and due to insufficient quantity of hydrological data. Furthermore, it should be noted that, even the most powerful high-performance computing clusters cannot provide a three-dimensional simulation of large areas of reservoirs. The areas in which simulation was made using the 1D, 2D and 3D models, are indicated in Fig. 1.

The 1D model describes the entire water area of the Kama reservoir from the Kama river observation station near the village Tyulkino up to the dam of the Kamskaya HPP. Simulations were done using HEC RAS [30]. Application of this 1D model made it possible to get necessary hydraulic data for the 2D model by analyzing information about the water inflows into the Kama reservoir and the operating regimes of the Kamskaya HPP.

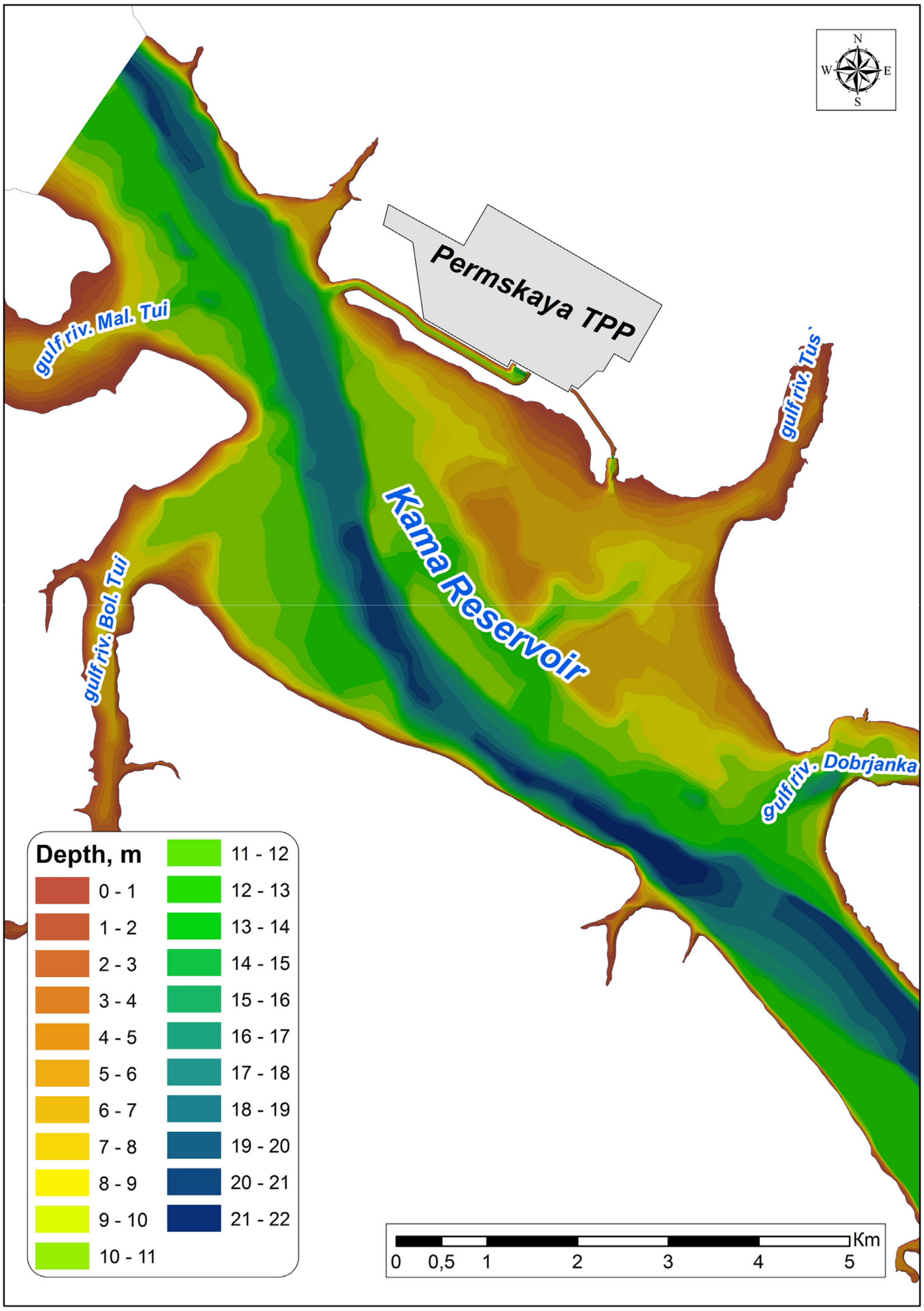

Fig. 2. Depth distribution map for the Kama reservoir in the area of the Permskaya TPP for a normal level of water at the Kamskaya hydropower plant (108.5 m.abs.)

The model of thermal pollution in the 2D formulation was applied to the particular part of the Kama reservoir (Ust-Garevaya village – Kamskaya HPP). There exists rich experience in using the models with shallow-water approximation (including the SMS code) for solving the problems of water reservoir hydrodynamics [30]. In this study, simulations were carried out with the licensed product SMSV 10.1 using the TUFLOW module [30,31]. The use of the 2D model allows us to qualitatively assess the velocity field distributions at different directions and speeds of the wind blowing over the part of the Kama reservoir near the Permskaya TPP (Fig. 6). The obtained results were used for the 3D numerical modeling of hydrothermal processes in the examined region of the Kama reservoir.

3.2. 3D simulations

The 3D hydrodynamical model was built for the part of the Kama reservoir with linear dimensions of 1000 m adjacent to the Permskaya TPP and including the water intake and water discharge zones. The ANSYS Fluent software package was used for 3D simulation on the computer cluster URAN located at the N.N. Krasovskii Institute of Mathematics and Mechanics (IMM UB RAS, Russia). The

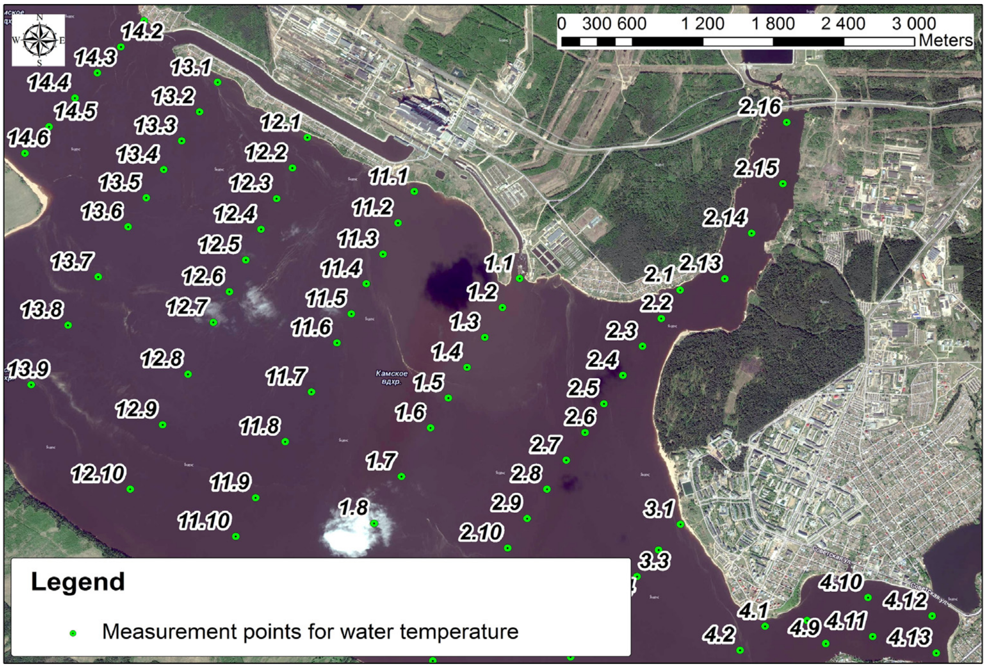

Fig. 3. Map with the measurement points location. Each point is denoted by two numbers, of which the first corresponds to the number of a measurement line, and the second to the point number along the line.

problem was solved using the non-stationary non-isothermal RANS approach in the framework of the $k-\varepsilon$ model for turbulence closure.

4. Governing equations

The mass balance and the momentum equations are written as

$$\frac{\partial \rho}{\partial t}+\frac{\partial}{\partial x_i}(\rho u_i)=0,$$

$$\frac{\partial}{\partial t}(\rho u_i)+\frac{\partial}{\partial x_j}(\rho u_i u_j)=-\frac{\partial p}{\partial x_i}+\frac{\partial}{\partial x_j}\left[\mu\left(\frac{\partial u_i}{\partial x_j}+\frac{\partial u_j}{\partial x_i}-\frac{2}{3}\delta_{ij}\frac{\partial u_l}{\partial x_l}\right)\right]+\frac{\partial}{\partial x_j}\left[\mu_t\left(\frac{\partial u_i}{\partial x_j}+\frac{\partial u_j}{\partial x_i}\right)-\frac{2}{3}\left(\rho k+\mu_t\frac{\partial u_l}{\partial x_l}\right)\delta_{ij}\right],$$

where ρ is the density, u_i is the Reynolds-averaged velocity components ($i=1,\ 2,\ 3$), p is the Reynolds-averaged pressure, and μ is the dynamic viscosity. The turbulent viscosity μ_t is the function of the kinematic turbulent energy k and the rate of energy dissipation ε: $\mu_t=\rho C_\mu k^2/\varepsilon$, where C_μ is a constant.

The equations for turbulent energy and its dissipation rate are given as

$$\frac{\partial}{\partial t}(\rho k)+\frac{\partial}{\partial x_i}(\rho k v_i)=\frac{\partial}{\partial x_j}\left[\left(\mu+\frac{\mu_t}{\sigma_k}\right)\frac{\partial k}{\partial x_j}\right]+G_k+G_b-\rho\varepsilon$$

$$\frac{\partial}{\partial t}(\rho\varepsilon)+\frac{\partial}{\partial x_i}(\rho\varepsilon v_i)=\frac{\partial}{\partial x_j}\left[\left(\mu+\frac{\mu_t}{\sigma_\varepsilon}\right)\frac{\partial \varepsilon}{\partial x_j}\right]+C_{1\varepsilon}\frac{\varepsilon}{k}(G_k+C_{3\varepsilon}G_b)-C_{2\varepsilon}\rho\frac{\varepsilon^2}{k},$$

where G_k denotes the generation of turbulent kinetic energy due to an average velocity gradients, G_b denotes the generation of turbulent kinetic energy due to buoyancy, $C_{1\varepsilon}$, $C_{2\varepsilon}$ are the constants, and σ_k, σ_ε are the turbulent Prandtl numbers k, ε respectively.

Stratification caused by changes in the water temperature is taken into account as follows:

$$G_b=g_i\left(\beta\frac{\mu_t}{Pr_t}\frac{\partial T}{\partial x_i}\right).$$

Simulation of the turbulent heat transfer is performed using the Reynolds-averaged model, which is similar to that of the turbulent momentum transfer. Hence, the energy equation is expressed as

$$\frac{\partial}{\partial t}(\rho E)+\frac{\partial}{\partial x_i}[u_i(\rho E+p)]=\frac{\partial}{\partial x_j}\left(\kappa_{eff}\frac{\partial T}{\partial x_j}+u_i(\tau_{ij})_{eff}\right),$$

where $E=ch+\frac{p}{\rho}$ denotes the total energy, $h=C_pT$ denotes the system enthalpy, κ_{eff} denotes the effective thermal conductivity, and $(\tau_{ij})_{eff}$ is the stress tensor deviator defined as

$$(\tau_{ij})_{eff}=\mu_{eff}\left(\frac{\partial u_j}{\partial x_i}+\frac{\partial u_i}{\partial x_j}\right)-\frac{2}{3}\mu_{eff}\frac{\partial u_k}{\partial x_k}\delta_{ij},$$

where $\mu_{eff}=\kappa_{eff}Pr/C_p$, is the effective viscosity, $\kappa_{eff}=\kappa+C_p\mu_t/Pr_t$ is the effective thermal conductivity, Pr is the Prandtl number, and κ is the thermal conductivity coefficient.

The validity of the $k-\varepsilon$ turbulent model used for simulation was verified by performing test calculations in the framework of a higher-order model – the Reynolds Stress Model (RSM) [32–34]. Since the difference between the obtained data does not exceed 5%, the $k-\varepsilon$ model has proved to be appropriate for further calculations.

The temperature dependence of density was assumed to be linear, and the Boussinesq approximation was applied as the most suitable one. The initial conditions were specified as the conditions of homogeneous temperature and velocity throughout the fluid volume, being equal to the temperature and velocity at the inlet to the computational domain.

For the parameters Pr_t, $G_{1\varepsilon}$, $C_{2\varepsilon}$, C_μ, σ_k, σ_ε the following values were taken [35]: $Pr_t=0.85$, $C_{1\varepsilon}=1.44$, $C_{2\varepsilon}=1.92$, $C_\mu=0.09$, $\sigma_k=1.0$, $\sigma_\varepsilon=1.3$. The dynamic viscosity was assumed to be $\mu=0.1\cdot 10^{-2}\ kg/(m\,s)$.

The spatial discretization scheme of the second-order accuracy was applied. Simulation of temporal evolution was carried out using an explicit second-order scheme.

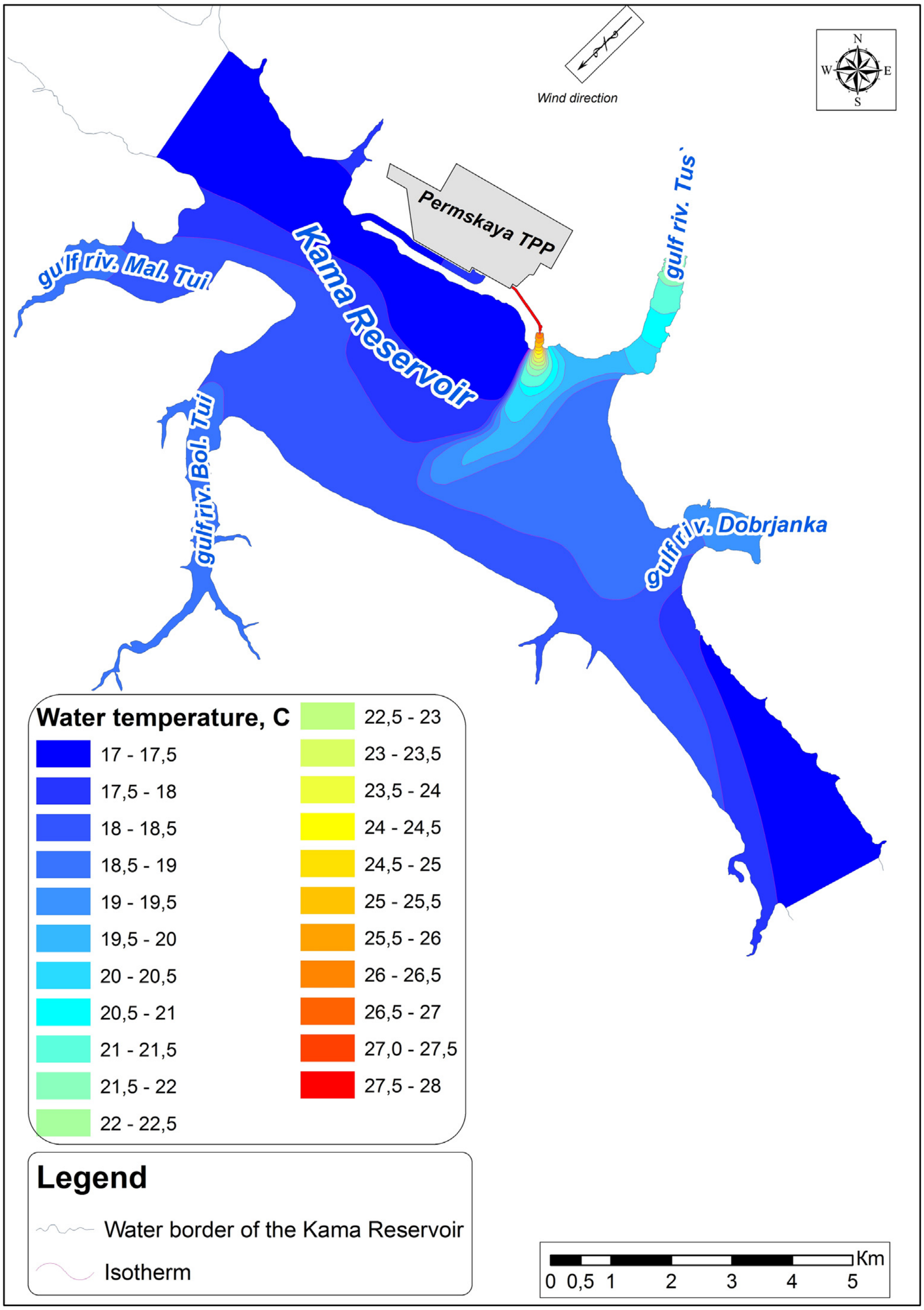

Fig. 4. Temperature distribution over the water surface of the Kama reservoir in July 17, 2014 (NE wind, air temperature 24–28 °C, two thermal power units were in operation, water discharge 40.5 m3/s, temperature of discharged water 27.8 °C).

5. Boundary conditions

The boundary conditions imposed on the edges of the computational domain were the no-slip and fixed temperature conditions specified at all rigid boundaries of the examined water basin

$$u_1 = u_2 = u_3 = 0, \quad T = T_0,$$

At the inlet to the computational domain the main flow velocity was assumed to have one nonzero component which was taken to be constant over the inlet cross-section, and the temperature was assumed to be equal to the background temperature of the water:

$$u_i = V_i, \quad T = T_0,$$

At water intake and water discharge points, the velocity and temperature were taken to be constant: $u_i = V_0,\ T = T_0$ at the water intake channel entrance and $u_i = V_1,\ T = T_1$ at the water discharge channel exit. To take into account the wind stress at the river surface, we used the formula $\tau = \rho_{air} C W^2$ presented in the work by Wu [36], where ρ_{air} is the air density, C is the dimensionless wind stress coefficient and W is the wind speed at 10 m above the water

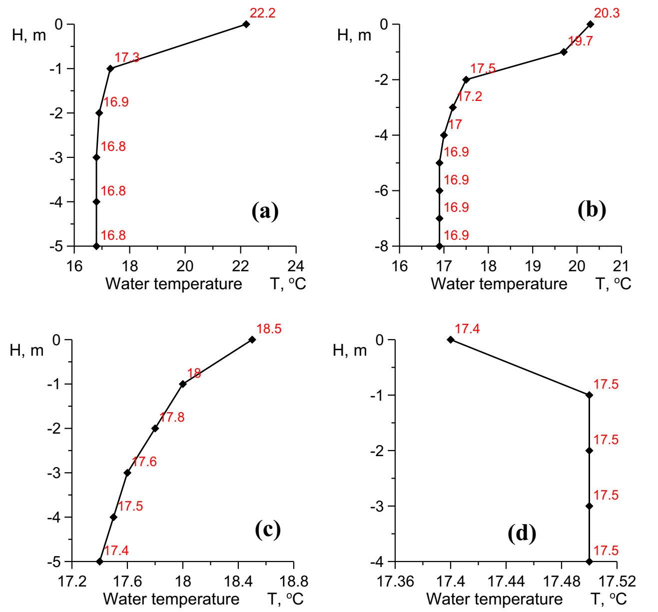

Fig. 5. Depth-wise temperature distribution along some measurement points in the area of the discharge channel of the Permskaya TPP for July 17, 2014. (a) – measurement point 1.2, (b) – measurement point 1.4, (c) – measurement point 2.7, (d) – measurement point 11.4 (location of measurement points is shown in Fig. 3).

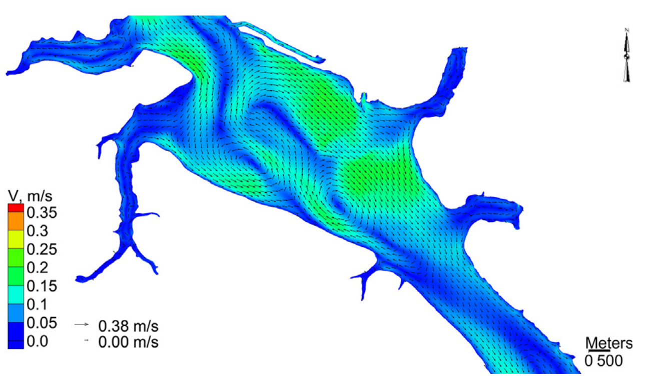

Fig. 6. Velocity vector field for the 2D model of the Kama reservoir in the area of the Permskaya TPP (first scenario).

surface. According to this formula, for 1 m/s < W < 15 m/s we have $C = 0.0005\,W^{0.5}$. In the calculations we used the value $C = 1.11e-03$ for $W = 5$ m/s and $C = 1.41e-03$ for $W = 8$ m/s.

The linear heat transfer law was used to take into account heating of the water surface by the surrounding air, and the heat transfer coefficient was selected based on the analysis of collected in-situ measurement data.

6. Meshing

A computational grid was generated by applying the Gambit 2.4 package of ANSYS Fluent. The number of nodes through the depth of the computational domain was taken to be 21. The non-uniform mesh was constructed using the bottom morphometric data obtained from the in-situ measurements taken in 2014. In a horizontal direction, the computational mesh consisted of tetragonal elements with the characteristic linear size of 20 m, which were uniformly distributed along the entire area, The mesh included 400 hundred thousands of nodes. A 3D picture of the mesh is given in Fig. 7.

To adapt the morphological data available in a coordinate-depth format to the capabilities of the Gambit mesh generator, the reservoir bottom morphology was represented as a set of simple geometrical objects of some specified resolution, which were then introduced into the file.

A special code was written to generate a batch file for the Gambit grid generator of the ANSYS Fluent package based on the data array, describing the reservoir bottom morphology. Thus, the complex geometry of the computational domain was considered.

Some preliminary studies were conducted to obtain a numerical solution to the problem of interest using the ANSYS Fluent. First, we obtained a stationary solution to the examined problem ignoring wind effects. Several hundreds of iterations were sufficient to achieve convergence of the solution. Then, using a non-stationary approach with the time step of 2 s we solved the problem taking into account the wind effect.

7. Model verification

The model was verified performing the calculations for the conditions of the Permskaya TTP recorded in July 2014 and comparing the results with the data of the in-situ measurements. All the related parameters are listed in Table 1. The computational period (under prescribed conditions) was 3 days.

The results obtained from the calculations were the temperature and velocity fields at different wind directions and velocities and the characteristics of the heated water discharge. Fig. 8 presents the temperature field in the upper surface layer of the Kama reservoir.

Fig. 9 shows the numerical results on the vertical distributions of temperature at some measurement lines, at which the in-situ measurements were conducted (Fig. 3). A comparison between the data from Figs. 5 and 9 demonstrates that the results of numerical modeling agree well with the results of the in-situ measurements, which supports the adequacy of the proposed model for further scenario calculations. This conclusion is also confirmed by the Fig. 10 where the numerical results obtained in the calculations are compared with the field measurements of the vertical distribution of water temperature in measurement points 1.3, 2.3, 3.7 and 11.3.

8. Numerical simulations for different scenarios

Further 3D simulations were carried out for two different scenarios to assess the impact of the Permskaya TPP on the Kama

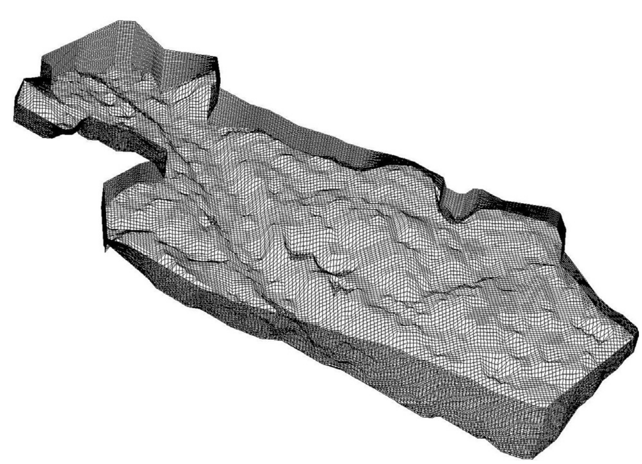

Fig. 7. Computational mesh. The vertical mesh size is shown at 50-fold magnification for perfect visualization, total area.

Table 1
Parameters used in the verification calculations and in the calculations for two main scenarios.

	Discharge flow rate (m^3/s)	Discharge water temperature (°C)	Number of power units	Intake flow rate at the station located 10 km upstream from the city of Dobryanka (m^3/sec)	Intake water temperature (°C)	Wind velocity and direction (m/s)
Verification calculations	40.5	27.8	2	850	17	5 (Northeast)
Scenario 1	63	32.4	3	850	21.8	8 (Northwest)
Scenario 2	63	32.4	3	850	21.8	8 (Southeast)

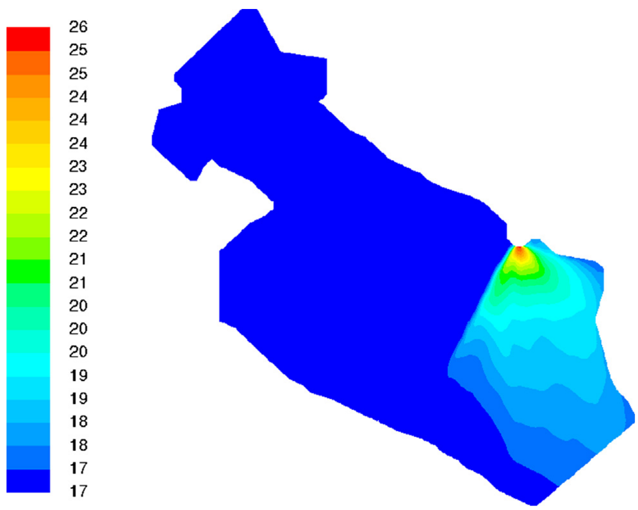

Fig. 8. Temperature field (°C) in the surface layer of the Kama reservoir obtained in the verification calculations.

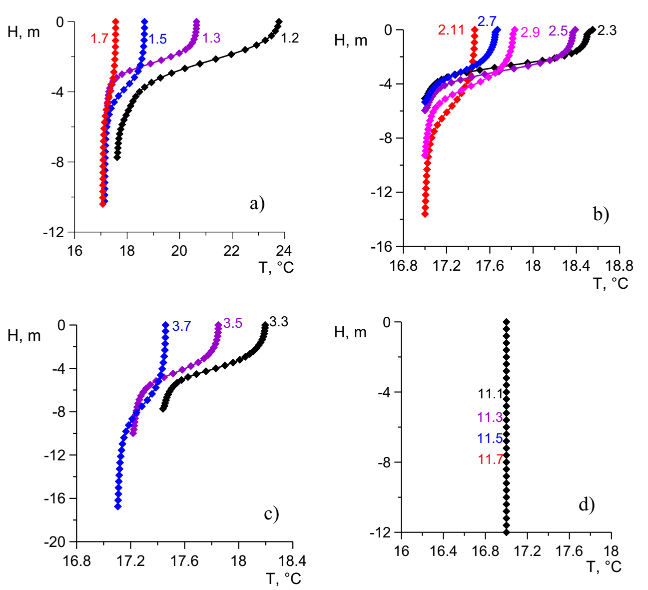

Fig. 9. Depth-wise distributions of temperature (°C) at different measurement lines (0-water surface corresponding to 108.5 m abs); (a) first measurement line, (b) second measurement line, (c) third measurement line, (d) eleventh measurement line.

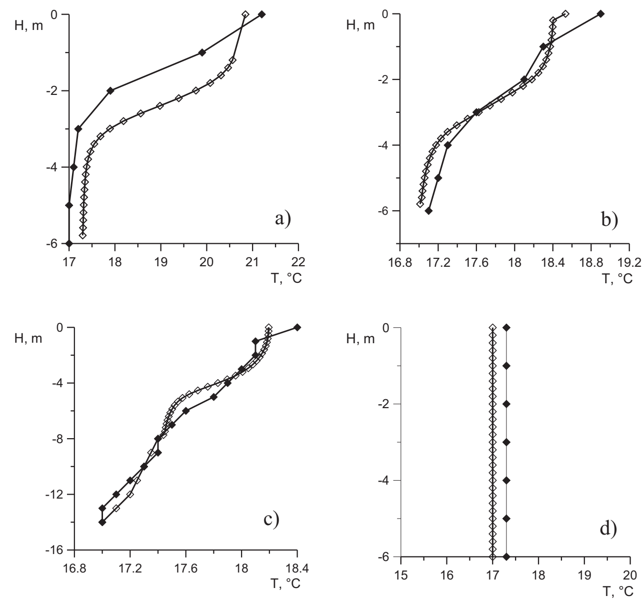

Fig. 10. Depth-wise distributions of temperature (°C) at the measurement points 1.3 (a), 2.3 (b), 3.7 (c), 11.3 (d). Empty symbols for the numerical data, filled symbols for the field measurements data.

reservoir. Below we present the results of computation for two scenarios for being most interesting from ecological and technological points of view.

At present, the Permskaya TPP includes 3 power generating units. Usually, 2 power units are in operation. For this operating regime we carried out the field measurements and verification calculations. The third power unit is put into operation only in the case of strong increase of power consumption, as usually happens in winter when the temperature of water is very low. In summer period this situation is rare but possible, and therefore it was also included in the list of scenarios for calculations.

8.1. The first scenario

The goal of calculations for the first scenario was to determine the maximum probable area of negative TPP impact on the reservoir (downstream) at a maximum fetch in the case of northern bearing winds, which are most probable in the area under consideration in July (see Fig. 11). The conditions arising from the implementation of this scenario are most unfavorable from the viewpoint of ecological safety usage of water for recreational purposes. The parameters for numerical simulation of this scenario are given in Table 1. The computational time (under the examined conditions) was 3 days.

8.2. The second scenario

The purpose of the calculations for this scenario was to evaluate the probability of the ingress of heated discharged water into the intake channel of the Permskaya TPP at extreme meteorological parameters. The technological parameters for this scenario were the same as in the first scenario. The hydrological and meteorological parameters were also the same as in the first scenario except for the wind direction which was south-east with the velocity of 8 m/s.

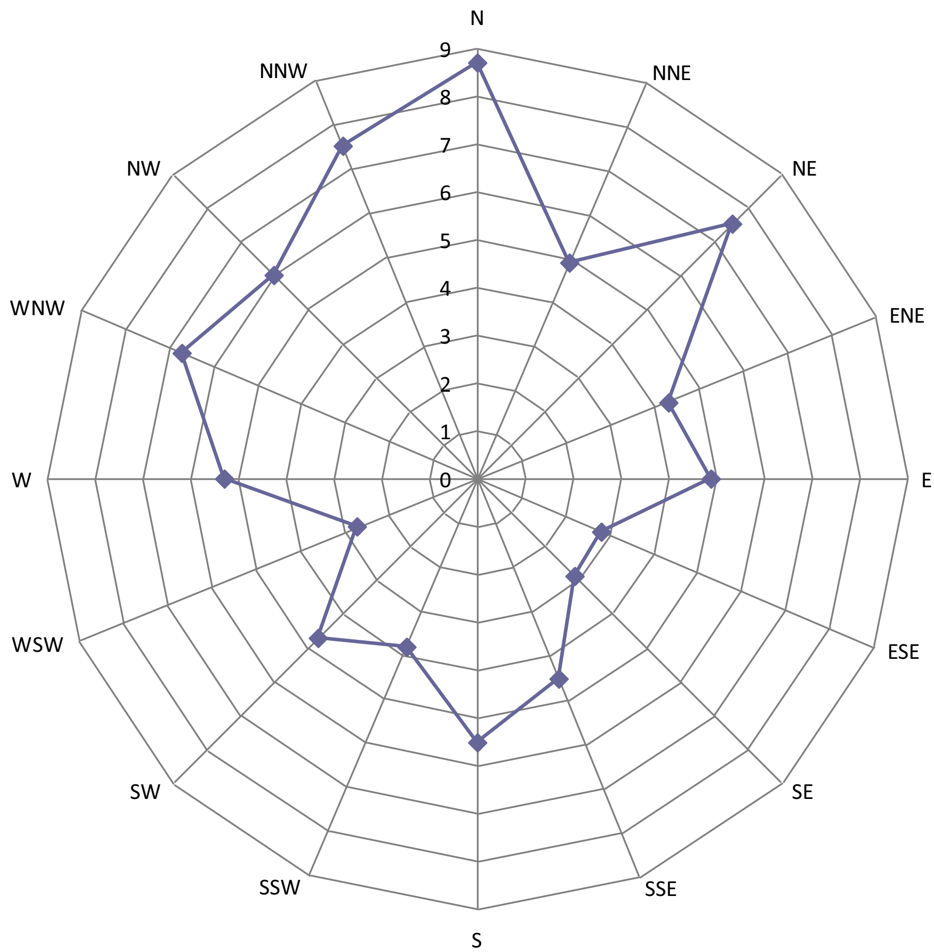

Fig. 11. Rose of wind in July 2008–2017 according to the observations made at Dobryanka meteostation.

9. Numerical results for different scenarios

9.1. The first scenario

The temperature field in the surface layer of water obtained in 3D calculations for the first scenario is shown in Fig. 12. Fig. 13a–d give water depth-wise temperature distributions at measurement lines 1, 2, 3 and 11 for the first scenario. It is seen from Fig. 13a, b,c that at measurement lines 1,2,3 the heated water flow is directed downstream, and a significant inhomogeneity of depth-wise temperature distribution is observed. At the intake channel entrance (Fig. 13d, measurement line 11), no inhomogeneities of temperature distribution through the depth of the reservoir and across its width are detected. However, it has been found that on the left bank of the reservoir, where a discharge channel is located, the temperature markedly increases downstream.

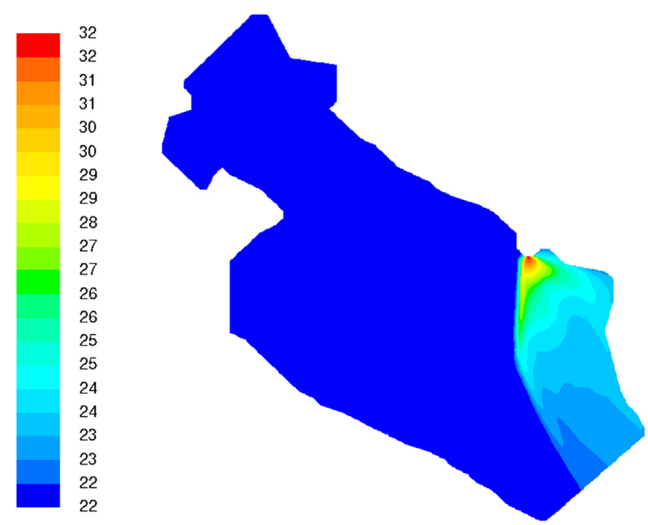

Fig. 12. Temperature field (°C) near the water surface 3 days after the discharge of heated waste water from the discharge channel. Scenario 1.

9.2. The second scenario

The most unfavorable, from a technological point of view, conditions arise within the second scenario, at extreme southwest winds. The ingress of discharge heated water into the intake channel of the Permskaya TPP may take place in this case. Fig. 14 presents the temperature field near the surface of water in the Kama reservoir.

Simulations show that under these conditions (at strong winds in the direction opposite to the course of a river) a 3D vortex is generated over a period of a few hours. The horizontal size of this vortex is equal to the distance between the joints of the intake and discharge channels with the Kama reservoir, and its vertical size is equal to the river depth. This vortex is responsible for the initiation of the heated water motion in the direction opposite to the

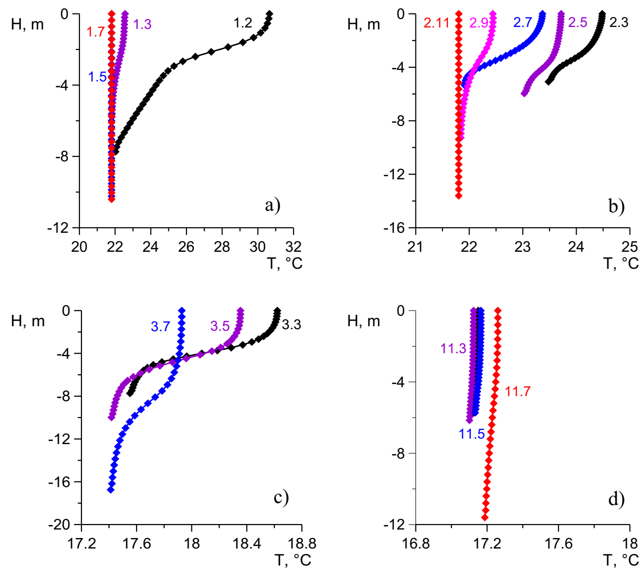

Fig. 13. Depth-wise temperature distributions at different measurement lines: (a) – first measurement line, (b) second measurement line, (c) third measurement line, (d) eleventh measurement line. Scenario 1.

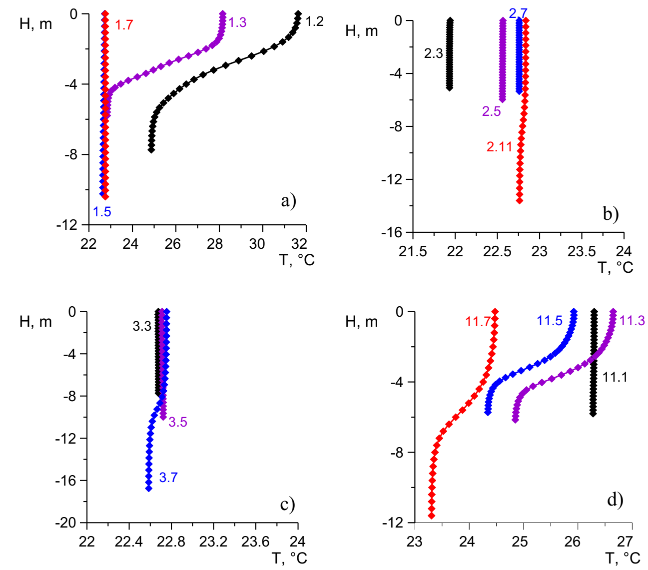

Fig. 15. Depth-wise temperature distributions at different measurement lines: (a) first measurement line, (b) second measurement line, (c) third measurement line, (d) eleventh measurement line. Scenario 2.

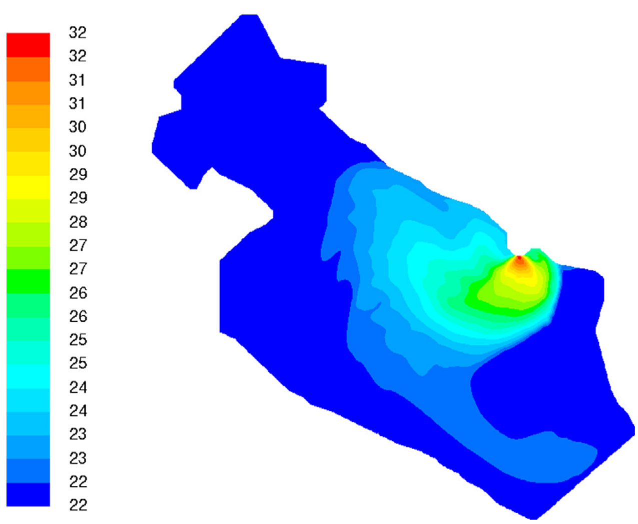

Fig. 14. Temperature field (°C) near the river surface 3 days after the ingress of heated water from the discharge channel. Scenario 2.

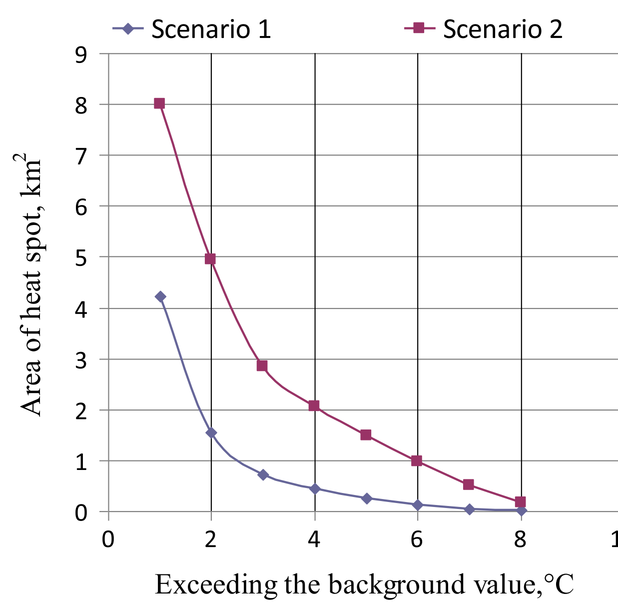

Fig. 16. The areas of zones where the water temperature exceeds the background temperature in the Permskaya TPP area of the Kama reservoir for different scenarios.

river flow. In this case, for less than twenty-four hours the heated water approaches the cooling water intake, which is extremely undesirable from the technological viewpoint. A significant depth-wise temperature inhomogeneity is also observed in this case (Fig. 15), and the temperature gradient has the highest value near the river bottom. The arrival of warm wastewater into the water intake channel has very unfavorable consequences, since it significantly reduces the efficiency of cooling, significantly increasing the intake of water. These adverse effects are most pronounced in the summer, the warmest period of the year.

The areas of the zones where the water temperature exceeds the background value in the Permskaya TPP area of the Kama reservoir are presented in Fig. 16 for two considered scenarios. As one can see, the area of the zone where the temperature exceeds the background value by 5 °C is about 1.5 km^2 for the second scenario and 0.3 km^2 for the first scenario.

10. Conclusions

Thermal pollution of water bodies is an unavoidable consequence of the operation of thermal or nuclear power plants. In order to minimize the negative effects of these plants, it is essential to assess the nature of dangerous zones. When the depth of the cooling water reservoirs exceeds 3–4 m, the wind is unable to provide vertical mixing and equalization of the water temperature over the depth of the reservoir. As a result, large masses of denser and colder water are formed in the bottom area of the reservoirs. Due to density stratification, these zones are very stable. Such zones play a crucial role in the formation of the thermal impact of large energy complexes on water bodies. At the same time, the traditional methods of calculations, ignoring density effects, in principle cannot describe these zones, which are very important for understanding the environmental consequences. The novelty of our paper is that we formulated the problem of modeling the zones of thermal impact on large reservoirs taking into account the influence of temperature on the density of water and the formation of corresponding density effects. The formulated problem was solved by analyzing the environmental and weather conditions of the part of the Kama reservoir near the Permskaya thermal power plant, one of the most powerful thermal plants in Europe.

Since the vertical temperature distribution in the cooling systems of thermal power plants is highly inhomogeneous, the computations to the required accuracy should be performed in the framework of 3D models. However, execution of such computations for large water bodies on the basis of the observation grids with strongly restricted resolution involves considerable difficulties due to the limited computing resources. In view of this fact, we implemented a combined scheme of computations, which includes the calculations based on 1D, 2D and 3D models. According to this scheme, the 1D model was constructed for the entire water body, the 2D model was used for the region of 30 km length adjoining the Permskaya TPP, and the 3D model was applied for the region of 10 km, which involved the intake and discharge channels of the TPP. A comparative analysis of the results of the 3D simulation and the experimental data demonstrated that the proposed scheme is quite efficient for simulation of temperature fields and estimation of their characteristics within the most unfavorable scenarios from the viewpoint of ecological and technological factors.

Summing up, we have considered two closely related problems, of which one is related to the estimation of risk of entering the warm water discharged from discharge channel to the intake channel, and the other is concerned with the calculation of the zones of thermal pollution of water reservoir is motivated by the need to estimate the influence of large power plants on the bio-resources of water reservoirs. Because of the peculiarities of technical use of these plants, the inflow of warm water from the discharge channel to the intake channel is a very negative factor. It may cause a great increase in the quantity of water supplies for technical purposes, which substantially worsens the economic indices of the TPP. These calculations allowed us to obtain a reasonable estimate of the zones of the possible thermal impact on the water reservoir at different operating regimes of the TPP and under different meteorological conditions. The calculations allowed to obtain the reasonable estimate of the zones of possible thermal impact to water reservoir at different regimes of TPP work and meteorological conditions.

Conflict of interest

No conflict of interest.

Acknowledgements

The study was supported by Russian Science Foundation (grant 17-77-20093).

References

[1] E.T. Hester, M.W. Doyle, Human impacts to river temperature and their effects on biological processes: a quantitative synthesis, J. Am. Water Resour. Assoc. 47 (2011) 571–587.
[2] C.E. Raptis, M.T.H. van Vliet, S. Pfister, Global thermal pollution of rivers from thermoelectric power plants, Environ. Res. Lett. 11 (10) (2016) 104011.
[3] M.T.H. van Vliet, J.R. Yearsley, F. Ludwig, S. Vögele, D.P. Lettenmaier, P. Kabat, Vulnerability of US and European electricity supply to climate change, Nat. Clim. Chang. 2 (2012) 676–681.
[4] N. Madden, A. Lewis, M. Davis, Thermal effluent from the power sector: an analysis of once-through cooling system impacts on surface water temperature, Environ. Res. Lett. 8 (2013) 035006.
[5] M.T.H. van Vliet, J.R. Yearsley, W.H.P. Franssen, F. Ludwig, I. Haddeland, D.P. Lettenmaier, P. Kabat, Coupled daily streamflow and water temperature modeling in large river basins, Hydrol. Earth Syst. Sci. 16 (2012) 4303–4321.
[6] F. Ling, G.M. Foody, H. Du, X. Ban, X. Li, Y. Zhang, Y. Du, Monitoring thermal pollution in rivers downstream of dams with Landsat ETM+ thermal infrared images, Rem. Sens. 9 (11) (2017) 1175.
[7] J. Wu, E.M. Buchak, J.E. Edinger, V.S. Kolluru, Simulation of cooling-water discharges from power plants, J. Environ. Manage. 61 (2001) 77–92.
[8] C.E. Raptis, S. Pfister, Global freshwater thermal emissions from steam-electric power plants with once-through cooling systems, Energy 97 (2016) 46–57.
[9] B. Mandelbrot, The Fractal Geometry of Nature, W.H. Freeman and Co., San Francisco, 1982.
[10] C.A. Fletcher, Computational techniques for fluid dynamics, Special Techniques for Differential Flow Categories, vol. 2. Springer, Berlin, 1988, p. 493.
[11] A.I. Tolstykh, Compact Difference Scheme and their Applications to Fluid Dynamics Problems, Nauka, Moscow, Russia, 1990.
[12] C.L. Parkinson, W.M. Washington, A large-scale numerical model of sea ice, J. Geophys. Res. 84 (1979) 311–337.
[13] S.H. Chieh, Two-dimensional numerical model of thermal discharges in coastal regions, J. Hydraul. Eng. 113 (8) (1987) 1032–1040.
[14] A.H.J. Abbaspour, P. Moghimi, K. Kayhan, Modeling of thermal pollution in coastal area and its economical and environmental assessment, Int. J. Environ. Sci. Technol. 2 (1) (2005) 13–26.
[15] A.A. Apukhtin, M.K. Klevannaya, K.A. Klevannyi, E.V. Smirnova, Computation of maximum water temperature in the Beloyarskoe Reservoir, Russ. Meteorol. Hydrol. 38 (12) (2013) 853–858.
[16] S.A. Lowe, F. Schuepfer, D.J. Dunning, Case study: three-dimensional hydrodynamic model of a power plant thermal discharge, J. Hydraul. Eng. 135 (4) (2009) 247–256.
[17] J. Prats, R. Val, J. Dolz, J. Armengol, Water temperature modeling in the Lower Ebro River (Spain): heat fluxes, equilibrium temperature, and magnitude of alteration caused by reservoirs and thermal effluent, Water Resour. Res. 48 (2012) W05523.
[18] R.V. Love, A. Wüest, M. Zappa, G. Fink, D. Bouffard, Tributaries affect the thermal response of lakes to climate change, Hydrol. Earth Syst. Sci. 22 (1) (2018) 31.
[19] A. Issakhov, Large eddy simulation of turbulent mixing by using 3D decomposition method, J. Phys. 318 (4) (2011) 42051.
[20] A. Issakhov, Mathematical modeling of the influence of thermal power plant on the aquatic environment with different meteorological condition by using parallel technologies. (Lecture Notes in Electrical Engineering), in: Power, Control and Optimization vol. 239, 2013, pp. 165–179.
[21] A. Issakhov, Mathematical modeling of thermal process to aquatic environment with different hydro meteorological conditions, Sci. World J. 2014 (2014) 678095.
[22] H. Tennekes, J.L. Lumley, A First Course in Turbulence, The MIT Press, Cambridge, Massachusetts, and London, England, 1972.
[23] M. Lesieur, O. Metais, P. Comte, Large Eddy Simulation of Turbulence, Cambridge University Press, New York, NY, USA, 2005.
[24] W. Rodi, G. Constantinescu, T. Stoesser, Large-eddy Simulation in Hydraulics, CRC Press, London, 2013.
[25] D.G. Kim, H.Y. Cho, Modeling the buoyant flow of heated water discharged from surface and submerged side outfalls in shallow and deep water with a cross flow, Environ. Fluid Mech. 6 (6) (2006) 501–518.
[26] T. Lyubimova, A. Lepikhin, Ya. Parshakova, V. Konovalov, A. Tiunov, Formation of the density currents in the zone of confluence of two rivers, J. Hydrol. 508 (2014) 328–342.
[27] A.P. Lepikhin, T.P. Lyubimova, Ya.N. Parshakova, A.A. Tiunov, Discharge of excess brine into water bodies at potash industry works, J. Min. Sci. 48 (2) (2012) 390–397.
[28] T. Lyubimova, A. Lepikhin, K. Tsiberkin, Ya. Parshakova, Self-oscillations in large storages of highly mineralized brines, Geophys. Res. Abstracts 16 (2014) EGU2014-10785.
[29] T. Lyubimova, A. Lepikhin, Ya. Parshakova, A. Tiunov, The risk of river pollution due to washout from contaminated floodplain water bodies during periods of high magnitude floods, J. Hydrol. 534 (2016) 579–589.
[30] G.W. Brunner, HEC-RAS, River Analysis System Hydraulic Reference Manual (CPD-69), Version 4.1, 411, 2010.
[31] TUFLOW User Manual. GIS Based 2D/1D Hydrodynamic Modelling. (Build 2008-08-AC), 475, 2008.
[32] M.M. Gibson, B.E. Launder, Ground effects on pressure fluctuations in the atmospheric boundary layer, J. Fluid Mech. 86 (1978) 491–511.
[33] B.E. Launder, Second-Moment Closure: Present... and Future?, Inter J. Heat Fluid Flow 10 (4) (1989) 282–300.
[34] B.E. Launder, G.J. Reece, W. Rodi, Progress in the development of a Reynolds-stress turbulence closure, J. Fluid Mech. 68 (3) (1975) 537–566.
[35] C. Gualtieri, A. Angeloudis, F.A. Bombardelli, S. Jha, T. Stoesser, On the values for the turbulent Schmidt number in environmental flows, Fluids 2 (2) (2017) 17.
[36] J. Wu, Wind stress and surface roughness at sea interface, J. Geophys. Res. 74 (1969) 444–453.